Single channel properties of recombinant $GABA_A$ receptors containing $\gamma 2$ or δ subtypes expressed with $\alpha 1$ and $\beta 3$ subtypes in mouse L929 cells

Janet L. Fisher* and Robert L. Macdonald *†‡

*Department of Neurology and †Department of Physiology, University of Michigan Medical Center, Ann Arbor, Michigan 48104–1687 USA

1. To determine their contributions to $GABA_A$ receptor (GABAR) channel properties, rat $\gamma 2L$ and δ subunits were acutely co-expressed with $\alpha 1$ and $\beta 3$ subtypes in mouse L929 fibroblasts to produce $\alpha 1\beta 3$, $\alpha 1\beta 3\delta$ or $\alpha 1\beta 3\gamma 2L$ GABAR isoforms.

2. With whole-cell recording, the $\alpha 1\beta 3$ isoform had relatively high sensitivity to GABA (EC_{50} 2·1 μM) and low maximum current amplitude. The $\alpha 1\beta 1\delta$ isoform had similar sensitivity to GABA (EC_{50} 2·8 μM) and low current amplitude. The $\alpha 1\beta 3\gamma 2L$ isoform had lower sensitivity to GABA (EC_{50} 11·6 μM) and higher maximum current amplitude.

3. The single channel conductance of $\alpha 1\beta 3$ channels was low (13 pS) compared with that of $\alpha 1\beta 3\delta$ and $\alpha 1\beta 3\gamma 2L$ channels (27 pS).

4. The single channel kinetic properties of the channels also differed. The $\alpha 1\beta 3\gamma 2L$ channel exhibited three open states, while the $\alpha 1\beta 3$ and $\alpha 1\beta 3\delta$ channels exhibited only two open states with mean dwell times similar to those of the two shorter open states of the $\alpha 1\beta 3\gamma 2L$ channel. All three channels exhibited at least five closed states. Bursts of $\alpha 1\beta 3\delta$ channels consisted primarily of only one or two openings, while those of $\alpha 1\beta 3$ channels contained multiple openings. $\alpha 1\beta 3\gamma 2L$ channels exhibited burst kinetics typical for native GABARs with several long openings per burst.

5. These results show that the $\alpha 1\beta 3$ heterodimer formed a GABA-sensitive channel with complex gating kinetics. Addition of a δ subunit to form the $\alpha 1\beta 3\delta$ heterotrimer altered the single channel conductance and the kinetic properties of the closed components, but did not affect the GABA sensitivity of the receptor nor the open state kinetics. In contrast, addition of a γ subunit ($\gamma 2L$ subtype) to produce the $\alpha 1\beta 3\gamma 2L$ heterotrimer affected the GABA sensitivity, channel conductance and kinetic properties of both open and closed states.

The $GABA_A$ receptor (GABAR) mediates the majority of fast inhibitory synaptic transmission in the central nervous system (CNS). GABARs are composed of pentameric combinations of $\alpha(1–6)$, $\beta(1–4)$ and $\gamma(1–4)$ or $\delta(1)$ subunit subtypes. Both $\beta 4$ and $\gamma 2$ subtypes have splice variants. The properties of GABARs depend upon their subunit and subtype composition (Sieghart, 1995). While the stoichiometry of GABARs has not been clearly determined, it is likely that most native GABARs are composed of combinations of α, β and either γ or δ subtypes. The regional expression of γ and δ subunit mRNAs in the mammalian brain is different, suggesting different roles for γ and δ subtype-containing GABARs. Messenger RNA for the γ subunit is widely expressed, with at least one subtype appearing in most brain regions and throughout development in the rat, while expression of mRNA for the δ subunit is more restricted, appearing principally in discrete regions of the post-natal rat brain; the hippocampal dentate gyrus, cerebellar granule cell layer and some regions of the thalamus (Shivers *et al.* 1989; Wisden, Laurie, Monyer & Seeburg, 1992; Laurie, Seeburg & Wisden, 1992*a*; Laurie, Wisden & Seeburg, 1992*b*). Structurally, γ and δ subunits share about 35% sequence similarity, about the same as between other GABAR subunit families (Shivers *et al.* 1989).

GABARs containing γ subunits have different pharmacological properties than those containing the δ subunit (Saxena & Macdonald, 1994; Krishek, Amato, Connolly, Moss & Smart, 1996). Incorporation of a γ subunit is required for benzodiazepine sensitivity and confers relative insensitivity to inhibition by zinc, cadmium, and hydrogen

‡To whom correspondence should be addressed at 1103 East Huron Street, Neuroscience Laboratory Building, Ann Arbor, MI 48104–1687, USA.

ions, compared with receptors containing a δ subunit (Saxena & Macdonald, 1994, 1996; Krishek *et al.* 1996). In general, incorporation of the δ subunit results in higher GABA affinity, slower and less complete whole-cell current desensitization and lower whole-cell current in transfected cells compared with receptors containing a $\gamma 2$ subtype (Saxena & Macdonald, 1994).

Although considerable study has focused on differences in the whole-cell pharmacological properties of recombinant GABARs composed of different subunit subtypes, less is known about the effect of subtype composition on the single channel properties of these receptors. Since the $\gamma 2$ subtype has the most widespread distribution in the CNS of the γ subunits, we studied the differences in the kinetic properties of GABARs containing either the $\gamma 2$L or δ subtypes. The $\alpha 1$ and $\beta 3$ subtypes were selected for co-expression because they are found at high levels in some regions of the brain that also express the δ or $\gamma 2$ subunits. We compared the properties of recombinant $\alpha 1\beta 3$, $\alpha 1\beta 3\gamma 2$L and $\alpha 1\beta 3\delta$ GABAR isoforms at both the whole-cell and single-channel levels to determine the influence of the γ and δ subunits on the functional properties of the GABAR.

METHODS

Transfection of L929 cells and selection of transfected cells

Full-length cDNAs for the rat $GABA_A$ subtypes $\alpha 1$ (Dr A. Tobin, University of California, Los Angeles), $\beta 3$ (Dr D. Pritchett, University of Pennsylvania), δ (Dr K. Angelides, Baylor College of Medicine) and $\gamma 2$L (F. Tan, University of Michigan) were subcloned into the pCMVNeo expression vector (Huggenvik, Collard, Stofko, Seasholtz & Uhler, 1991) and transfected into the mouse fibroblast cell line L929 (American Type Culture Collection, Rockville, MD, USA). For selection of transfected cells, the plasmid pHook™-1 (Invitrogen, San Diego, CA, USA) containing cDNA encoding the surface antibody sFv was also transfected into the cells. L929 cells were maintained in Dulbecco's modified Eagle medium (DMEM) plus 10% heat-inactivated horse serum, 100 i.u. ml^{-1} penicillin and 100 $\mu g\ ml^{-1}$ streptomycin. Cells were passaged by a 5 min incubation with 0·5% trypsin, 0·2% EDTA solution in phosphate-buffered saline (10 mM Na_2HPO_4, 0·15 mM NaCl, pH at 7·3).

The cells were transfected using a modified calcium phosphate precipitation technique (Chen & Okayama, 1987; Angelotti, Uhler & Macdonald, 1993). GABAR subunit plasmids were added to the cells in 1 : 1 ratios of 4 μg each plus 8 μg of the plasmid encoding sFv. Following a 4–6 h incubation at 3% CO_2, the cells were treated with a 15% glycerol solution in BBS buffer (50 mM Bes, 280 mM NaCl and 1·5 mM Na_2HPO_4) for 30 s. The selection procedure for sFv antibody expression was performed 20–28 h later as described in Greenfield, Sun, Neelands, Burgard, Donnelly & Macdonald (1997). Briefly, the cells were passaged and mixed with 5 μl of magnetic beads coated with hapten (approximately $7{\cdot}5 \times 10^5$ beads; Invitrogen). Following 30–60 min of incubation to allow the beads to bind to positively transfected cells, the beads and bead-coated cells were isolated using a magnetic stand. The selected cells were resuspended into DMEM, plated onto 35 mm culture dishes and used for recording 18–28 h later.

Recording solutions and techniques

For both whole-cell and outside-out patch recording the external solution consisted of (mM) 142 NaCl, 8·1 KCl, 6 $MgCl_2$, 1 $CaCl_2$, 10 glucose and 10 Hepes with pH at 7·4 and osmolarity adjusted to 295–305 mosmol (l solution)$^{-1}$. Recording electrodes were filled with an internal solution (mM): 153 KCl, 1 $MgCl_2$, 5 K-EGTA, 10 Hepes and 2 MgATP with pH at 7·4 and osmolarity adjusted to 295–305 mosmol (l solution)$^{-1}$. These solutions provided an equilibrium potential for Cl^- near 0 mV. Patch pipettes were pulled from thick-walled borosilicate glass with an internal filament (World Precision Instruments, Pittsburgh, PA, USA) on a P-87 Flaming Brown puller (Sutter Instrument Co., San Rafael, CA, USA) and fire-polished to a resistance of 5–10 MΩ, with a mean of 6 MΩ. Mean access resistance was 12 MΩ. Due to the large maximal peak currents (> 2000 pA) recorded from the $\alpha 1\beta 3\gamma 2$L isoform, series resistance compensation was performed to compensate for the series resistance error in holding potential during the peak currents. However, because of the small maximal peak currents (< 300 pA for $\alpha 1\beta 3$ and < 100 pA for $\alpha 1\beta 3\delta$) recorded from the other isoforms, series resistance compensation should not have significantly altered peak currents and was not performed. For single-channel recordings the pipettes were coated with Q-dope (GC Electronics, Rockford, IL, USA). For whole-cell recordings, drugs were applied to cells using a 'multi-puffer' system with a 10–90% rise time of 70–150 ms (Greenfield & Macdonald, 1996). At least 90 s were allowed between successive GABA applications to allow removal of GABA from the bath and recovery of the cell from desensitization. For patch recordings drugs were applied using a pressure ejection pipette. Currents were recorded with a List EPC-7 (Darmstandt, Germany) patch clamp amplifier and stored on Beta tape. All experiments were performed at room temperature (20–23 °C).

Analysis of whole-cell currents

Whole-cell currents were analysed off-line using the programs Axotape (Axon Instruments), Prism (Graphpad, San Diego, CA) and Clampfit (Axon Instruments). Concentration–response curves were fitted with a four-parameter logistic equation:

$$\text{current} = \frac{\text{maximum current}}{1 + 10^{(\log EC_{50} - \log[GABA])n)}}.$$

Statistical tests were performed using the Instat program (Graphpad). Comparisons of the receptor properties were performed with one-way analysis of variance and Tukey–Kramer multiple comparisons test with a statistical significance level of 0·05.

Analysis of single-channel currents

Single-channel recordings were digitized using Axotape and analysed using pCLAMP6 (Axon Instruments) and Interval5 (Dr Barry S. Pallotta, University of North Carolina at Chapel Hill). For analysis, the data were digitized at 20 kHz and filtered at 2 kHz. Intervals were measured with a 50% threshold detection method. Subconductance levels were rarely observed (≤ 1% of openings) but were included in the analysis if they reached the 50% threshold. To reduce errors due to multi-channel patches, recordings were only included in the kinetic analysis if overlaps of simultaneous openings occurred for less than 1% of the openings. Overlapped openings and bursts were not included in the kinetic analysis. The presence of multiple channels would decrease the apparent duration of the longer closed components, but would have no effect on the open state or burst properties. Duration histograms were constructed as described by Sigworth & Sine (1987) and fitted by a maximum likelihood method. The number of exponential functions required

to fit the distribution was increased until additional components did not significantly improve the fit as determined by the log–likelihood ratio test (Horn, 1987; McManus & Magleby, 1988). Intervals with durations less than 1·5 times the system dead-time were displayed in the histograms but were not included in the fit. For the definition of bursts the two shortest closed components were considered as intraburst closures. A critical gap for each patch was calculated from the closed interval distribution to equalize the proportion of misclassified events (Colquhoun & Sakmann, 1985).

All results are quoted as means ± S.E.M. unless otherwise stated.

RESULTS

Whole-cell α1β3, α1β3δ, and α1β3γ2L GABAR currents

Whole-cell currents were evoked by GABA from fibroblasts transfected with vectors containing rat GABAR subunit cDNAs to produce α1β3, α1β3δ or α1β3γ2L isoforms (Fig. 1). Peak whole-cell currents increased in a concentration-dependent manner, but whole-cell currents from the three isoforms showed different characteristics. α1β3 currents had relatively low maximum peak amplitudes and desensitized rapidly and completely, with desensitization apparent at concentrations of GABA below the EC_{50}. The deactivation rate of the α1β3 currents was particularly slow following the removal of high concentrations of GABA and in some cases a transient increase in current was observed before returning to baseline. The rapid desensitization rate and slow recovery rate were also observed with α1β2 channels by Verdoorn, Draguhn, Ymer, Seeburg & Sakmann (1990). This could be indicative of a rapid recovery from desensitization for this isoform. α1β3δ currents also tended to be small in amplitude but showed little desensitization, even at saturating GABA concentrations or with extended application time. A mean of 92 ± 5% ($n = 4$) of the α1β3δ current remained at the end of a 5 min application of 600 μM GABA. α1β3γ2L currents were relatively larger in amplitude and desensitized more rapidly than α1β3δ currents, with desensitization becoming apparent only at GABA concentrations above the EC_{50}. This is in contrast to the findings of Dominguez-Perrot, Feltz & Poulter (1996), who found that α1β3γ2 currents desensitized more rapidly than α1β3 currents.

Maximum whole-cell currents

The three isoforms differed in the mean maximum currents evoked by saturating concentrations of GABA. The α1β3γ2L isoform produced the highest peak currents with a mean of 2239·5 ± 597·1 pA ($n = 8$). The α1β3 and α1β3δ isoforms produced currents with a mean of 270·4 ± 53·4 pA ($n = 10$) and 89·1 ± 17·6 pA ($n = 11$), respectively. The magnitudes of α1β3 and α1β3δ currents were significantly smaller than α1β3γ2L currents, but were not significantly different from each other. A difference in maximum current could be related to the underlying single-channel kinetic properties, but could also reflect a difference in the amount of membrane surface expression of functional recombinant receptors.

Sensitivity to GABA

GABA concentration–response relationships for all three isoforms were normalized to the maximum current for each cell and fitted by a four-parameter logistic equation (Fig. 2). The α1β3 and α1β3δ isoforms were the most sensitive to

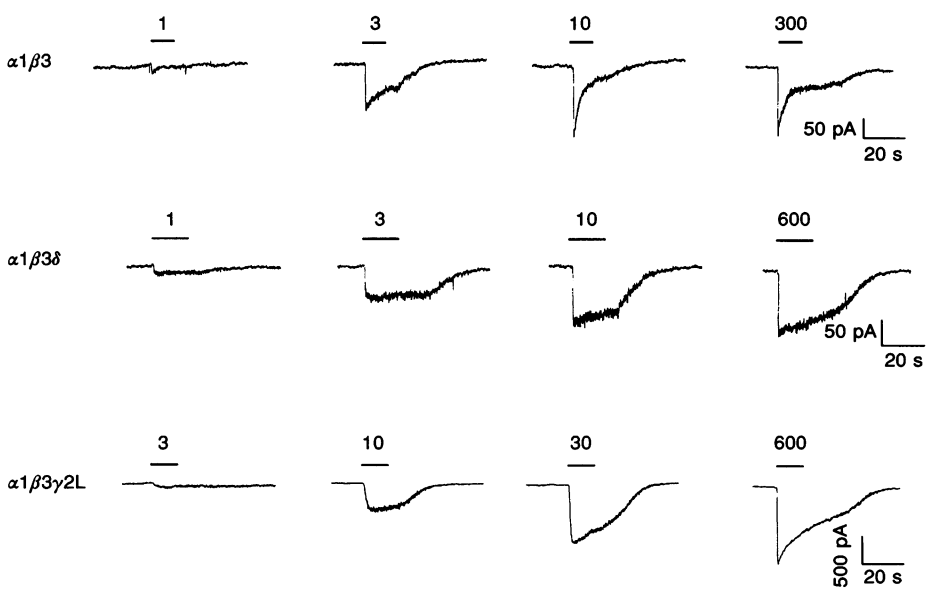

Figure 1. Whole-cell current responses to GABA

Whole-cell GABAR current records from transfected L929 cells. Peak currents increased in a concentration-dependent manner. Traces shown were from a single fibroblast for each isoform. GABA was applied as indicated by the bar for 10–15 s to cells held at −50 mV at the concentrations quoted above the bar in μM.

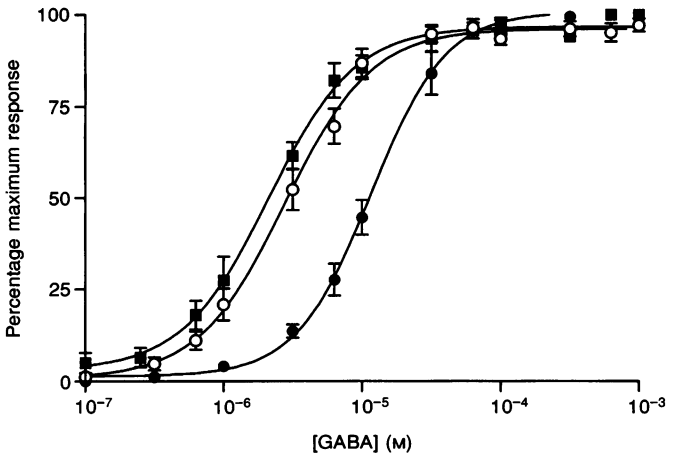

Figure 2. GABA concentration–response relationships

Peak currents evoked by varying GABA concentrations were measured for each isoform. $\alpha1\beta3$, ■; $\alpha1\beta3\delta$, ○ and $\alpha1\beta3\gamma2L$, ●. Symbols represent the means ± S.E.M. of normalized concentration–response data. These data were fitted with a four-parameter logistic equation. EC_{50}s for these fits were 2·1 μM ($\alpha1\beta3$, $n = 7$), 2·8 μM ($\alpha1\beta3\delta$, $n = 11$) and 11·6 μM ($\alpha1\beta3\gamma2L$, $n = 8$). Slopes of the fits were 1·4 for $\alpha1\beta3$, 1·4 for $\alpha1\beta3\delta$ and 1·6 for $\alpha1\beta3\gamma2L$ receptors.

GABA. The $\alpha1\beta3$ isoform had a mean EC_{50} of 2·2 ± 0·3 μM ($n = 7$) from fits of data from individual cells, and addition of the δ subunit to produce the $\alpha1\beta3\delta$ isoform did not significantly alter GABA sensitivity, with a mean EC_{50} of 3·5 ± 0·6 μM ($n = 11$). The $\alpha1\beta3\gamma2L$ isoform, however, was significantly ($P \leqslant 0{\cdot}05$) less sensitive to GABA, with a mean EC_{50} of 13·2 ± 1·8 μM ($n = 8$).

Hill slopes of the fits of the individual concentration–response curves were greater than one and were not significantly different among the isoforms, with mean Hill slopes of 1·58 ± 0·21 ($\alpha1\beta3$), 1·77 ± 0·18 ($\alpha1\beta3\delta$) and 1·76 ± 0·12 ($\alpha1\beta3\gamma2L$). Hill slopes greater than one have been previously reported for many native and recombinant GABARs (Macdonald & Angelotti, 1993).

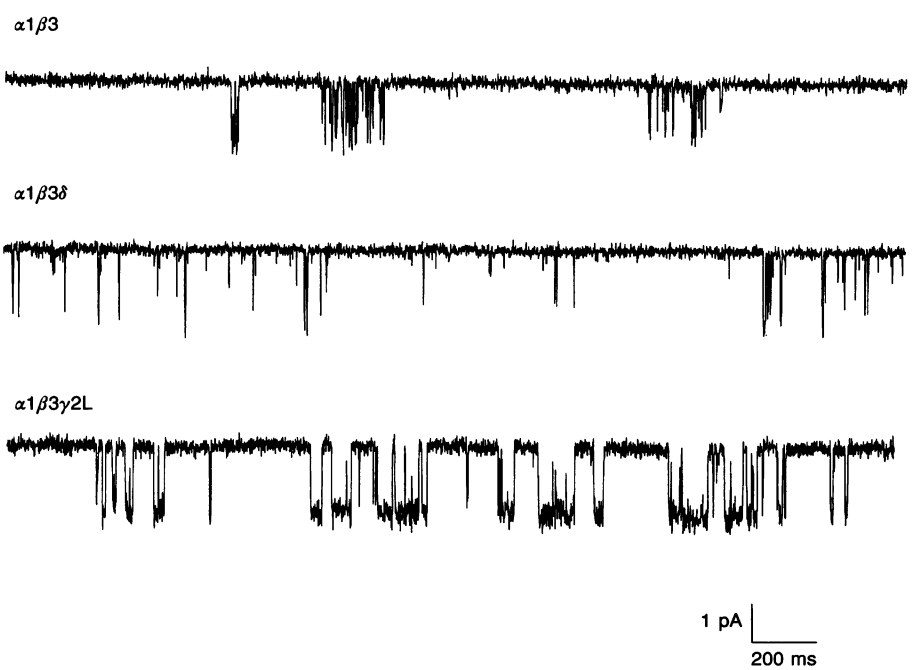

Figure 3. Single-channel characteristics

Single-channel GABAR currents were obtained from outside-out patches. Traces shown were continuous 2 s recordings from patches in response to 3 μM ($\alpha1\beta3$, $\alpha1\beta3\delta$) or 10 μM GABA ($\alpha1\beta3\gamma2L$). In this and all subsequent figures, channel openings are downward. For $\alpha1\beta3\delta$ and $\alpha1\beta3\gamma2L$ patches were held at −70 mV, and for $\alpha1\beta3$ recordings the holding potential was −100 mV. For display the data were sampled at 300 μs point^{-1} and filtered at 500 Hz.

α1β3, α1β3δ and α1β3γ2L GABAR single-channel currents

For comparison of the single channel properties of these receptors, GABA was applied to outside-out patches pulled from transfected fibroblasts. The kinetic properties of the channels were compared at GABA concentrations near the EC_{50}s for each isoform (3 μM GABA for α1β3 and α1β3δ and 10 μM GABA for α1β3γ2L receptors). Single-channel conductance and kinetic properties differed among the channels (Fig. 3). α1β3 channel openings had a lower amplitude than those of the α1β3δ and α1β3γ2L channels. α1β3 channel openings were relatively short in duration and were separated into widely spaced bursts and clusters of openings. α1β3δ channel openings were also relatively short in duration, but openings tended to occur in groups of one or two, rather than in longer bursts. The α1β3γ2L channel exhibited many longer duration openings and these openings tended to occur in a pattern of closely grouped bursts and clusters.

Single-channel conductance. The amplitudes of single-channel openings for each of the three channels were measured at holding potentials ranging from −90 to +90 mV and were fitted using linear regression analysis to determine single-channel conductance (Fig. 4). From fits of individual patches the mean conductance of α1β3 channel openings was 13·3 ± 0·4 pS ($n = 5$). The conductance of α1β3 channel openings was significantly lower than that of α1β3δ (26·7 ± 0·7 pS, $n = 5$) and α1β3γ2L (27·1 ± 0·8 pS, $n = 6$) channel openings, which were not significantly different from each other. The main conductance level of the α1β3 channel was similar to that reported by other investigators for αβ heterodimers (11–17 pS) (Verdoorn *et al.* 1990; Porter, Angelotti, Twyman & Macdonald, 1992; Angelotti & Macdonald, 1993). The mean reversal potentials for the individual patches were near zero for all channels, −0·9 ± 0·4 mV (α1β3), −0·4 ± 0·6 mV (α1β3δ), and 1·7 ± 0·8 mV (α1β3γ2L), as predicted for a chloride ion selective channel.

Single-channel kinetic properties. The kinetic properties of the channel openings and closings of the three channels were compared by constructing open and closed duration histograms from data obtained during long (2–10 min) applications of GABA. Patches were voltage clamped at −70 mV for α1β3δ and α1β3γ2L channels, but because of

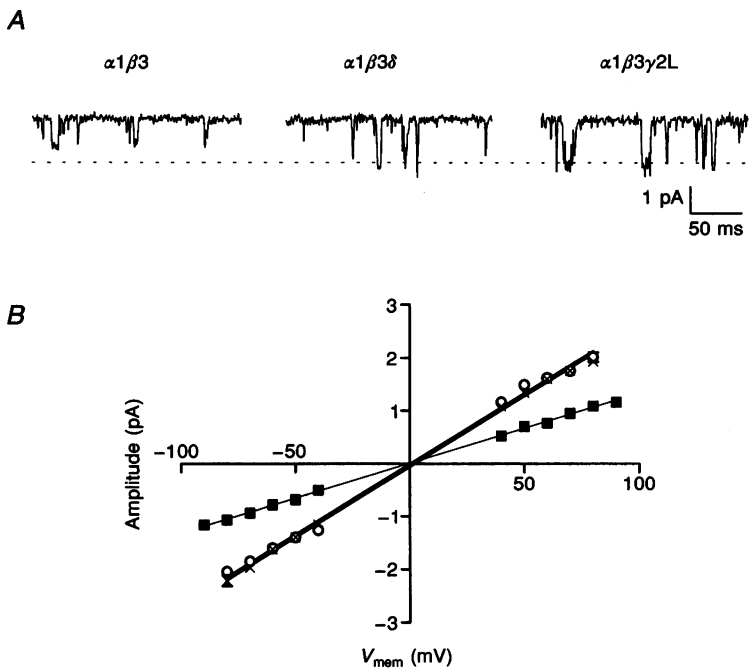

Figure 4. Single-channel conductance

A, α1β3 channels had a lower single-channel amplitude than α1β3δ and α1β3γ2L channels. Traces shown are continuous 200 ms recordings from outside-out patches in response to GABA. The dashed line indicates the main conductance state of α1β3δ and α1β3γ2L channels and was 1·88 pA from baseline. Patches were held at −70 mV. *B*, the single-channel current–voltage relationships of the main conductance levels were linear for all channels. α1β3 (■); α1β3δ (○) and α1β3γ2L (×). Points shown are mean amplitudes ± S.E.M. Where error bars are not apparent they are smaller than the symbol. Linear regression lines were drawn through mean points. The slopes of these lines were 13·3 pS (α1β3, $n = 5$), 26·7 pS (α1β3δ, $n = 5$), and 26·8 pS (α1β3γ2L, $n = 6$). The reversal potentials were −0·66 mV (α1β3), 0·40 mV (α1β3δ) and 2·2 mV (α1β3γ2L).

Table 1. Kinetic properties

	α1β3	α1β3δ	α1β3γ2L
Number of patches	6	7	8
NP_o (×100)	0·28 ± 0·07	0·69 ± 0·27	3·74 ± 0·81**
Mean open time (ms)	0·461 ± 0·044	0·428 ± 0·051	2·10 ± 0·28***
Mean shut time (ms)	230·01 ± 42·0	151·22 ± 52·91	69·95 ± 17·39†
Mean burst duration (ms)	2·48 ± 0·51	1·15 ± 0·26	7·32 ± 1·11**
Mean openings/burst	2·70 ± 0·27	1·55 ± 0·06**	3·36 ± 0·23

* significant difference from both of the other isoforms, ** $P \leq 0{\cdot}01$, *** $P \leq 0{\cdot}001$. † significantly different from α1β3 channel only ($P \leq 0{\cdot}05$).

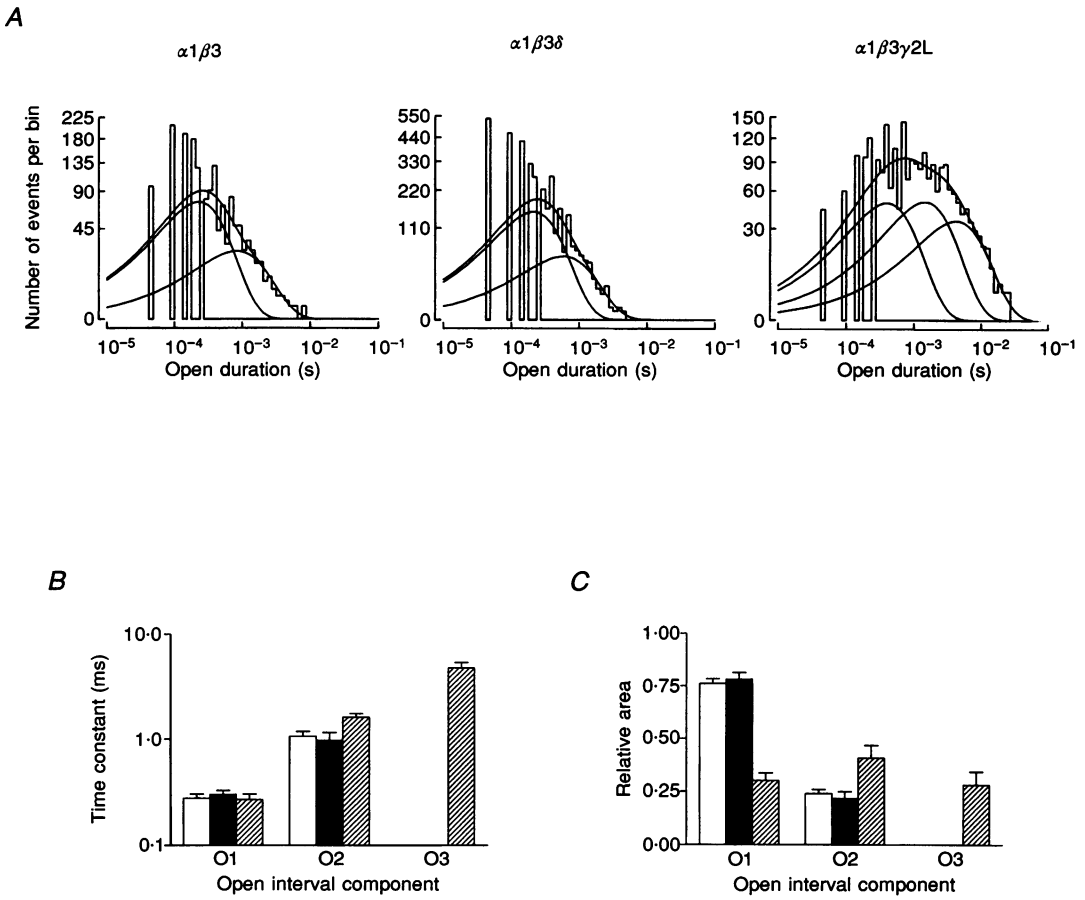

Figure 5. Open interval kinetic properties

A, duration histograms of open intervals from individual patches for the three channels were fitted with the sum of two (α1β3, α1β3δ) or three (α1β3γ2L) exponential functions. For the α1β3 histogram shown, the individual components had time constants (and relative areas) of 0·26 ms (0·747) and 0·963 ms (0·253) with 1583 open intervals. For the α1β3δ histogram shown, the individual components had time constants (and relative areas) of 0·24 ms (0·743) and 0·68 ms (0·256) with 3472 open intervals. For the α1β3γ2L histogram shown, the individual components had time constants (and relative areas) of 0·46 ms (0·365), 1·67 ms (0·272) and 4·84 ms (0·262) with 2333 open intervals. *B*, the mean time constants of the open interval components from the open duration histograms for individual patches were taken. Bars represent means + S.E.M. for patches for the three isoforms (□, α1β3, $n = 6$; ■, α1β3δ, $n = 7$; ▨, α1β3γ2L, $n = 8$) patches. O1 represents the shortest component, O2 the second longest and O3 the longest open interval component. Only two open states (O1 and O2) were observed for the α1β3 and α1β3δ isoforms. *C*, the mean relative proportions of the open interval components were taken for individual patches. Symbols as *B*, bars represent means + S.E.M.

its low conductance, recordings of $\alpha1\beta3$ channels were made at −100 mV. While no obvious differences in channel properties were apparent between holding potentials of −70 mV and −100 mV, it is possible that the difference in holding potential may have had subtle effects on the kinetic properties of the $\alpha1\beta3$ channel.

The open probability (NP_o) of $\alpha1\beta3\gamma2L$ channels was about 5-fold greater than that of the $\alpha1\beta3\delta$ channels and about 13-fold greater than that of the $\alpha1\beta3$ channels (Table 1). This is consistent with the relative amplitude of the steady-state whole-cell currents from these channels at EC_{50} GABA concentrations. The number of channels in the patches (N) was unknown. Therefore, differences in the measured open probability could also be due to differences in the number of active channels. Although $\alpha1\beta3$ and $\alpha1\beta3\delta$ peak whole-cell currents were similar, the large degree of desensitization observed with $\alpha1\beta3$ currents could account for the reduced channel activity during steady-state recording.

Open state properties. The mean open times of the $\alpha1\beta3$ and $\alpha1\beta3\delta$ channels were similar, while that of the $\alpha1\beta3\gamma2L$ channel was almost 5-fold longer (Table 1). Open interval histograms were fitted best with the sum of two ($\alpha1\beta3$, $\alpha1\beta3\delta$) or three ($\alpha1\beta3\gamma2L$) exponential functions (Fig. 5*A*). The time constants of the two shorter open states were similar for all three channels (Fig. 5*B*). For the $\alpha1\beta3$ and $\alpha1\beta3\delta$ channels, the relative proportions of the open states were also similar (Fig. 5*C*). For the $\alpha1\beta3\gamma2L$ channel, most of the openings were to the two longer open states (O2 and O3). The differences in the open state properties were consistent with the differences in mean open times (Table 1).

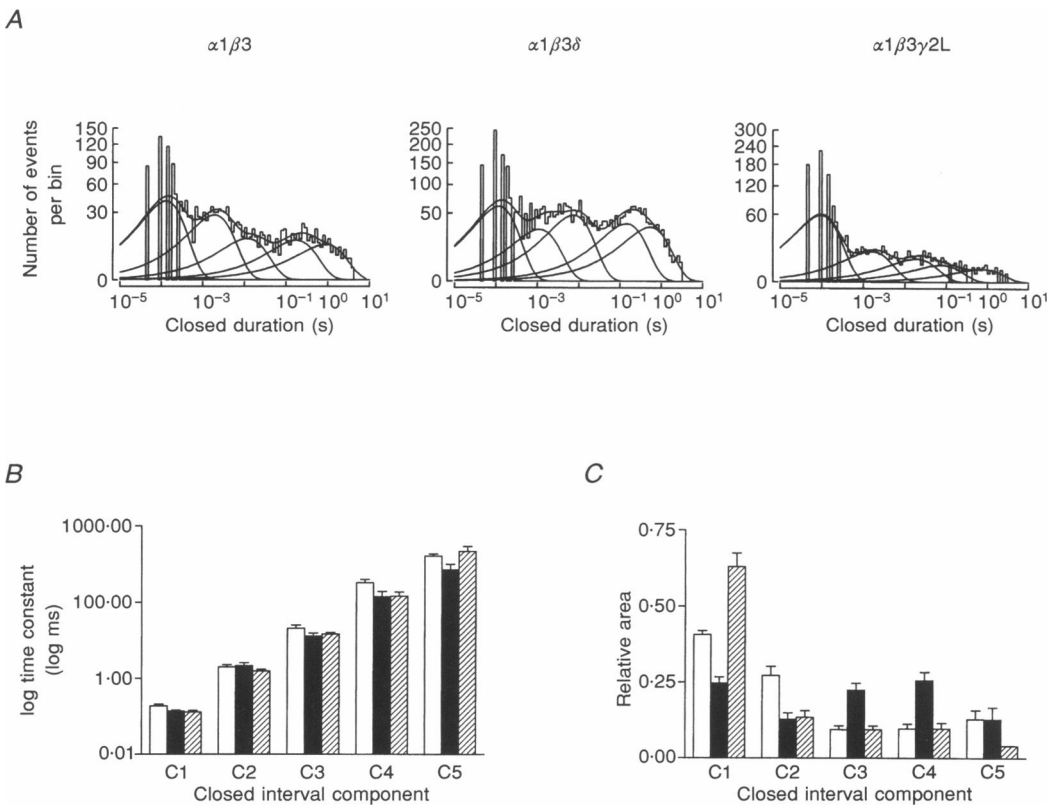

Figure 6. Closed interval kinetic properties

A, duration histograms of closed intervals from individual patches for the three channels were fitted with the sum of five exponential functions. For the $\alpha1\beta3$ histogram shown, the individual components had time constants (and relative areas) of 0·15 ms (0·413), 2·21 ms (0·282), 13·6 ms (0·114), 201·8 ms (0·105), and 1008·3 ms (0·084) with 1583 closed intervals. For the $\alpha1\beta3\delta$ histogram shown, the individual components had time constants (and relative areas) of 0·14 ms (0·294), 1·30 ms (0·142), 8·49 ms (0·232), 162·3 ms (0·176) and 605·9 ms (0·155) with 3472 closed intervals. For the $\alpha1\beta3\gamma2L$ histogram shown, the individual components had time constants (and relative areas) of 0·11 ms (0·698), 1·76 ms (0·145), 21·5 ms (0·084), 85·8 ms (0·045) and 855·0 ms (0·026) with 1177 closed intervals. *B*, the mean time constants for the closed components from the closed duration histograms for individual patches are plotted. Bars represent means + S.E.M. for patches for the three isoforms (□, $\alpha1\beta3$, $n = 6$; ■, $\alpha1\beta3\delta$, $n = 7$; ▨, $\alpha1\beta3\gamma2L$, $n = 8$). Components were numbered with increasing mean duration, so that C1 represents the shortest duration component, and C5 the longest duration component. *C*, the mean relative areas of the five closed components from the closed duration histograms were taken for individual patches. Bars represent means + S.E.M. Symbols as *B*.

Closed state properties. The mean shut times of the $\alpha1\beta3$ and $\alpha1\beta3\delta$ channels were similar, while that of the $\alpha1\beta3\gamma2L$ channel was somewhat shorter (Table 1). Closed interval histograms for all three channels were fitted best with the sum of five exponential functions with similar time constants (Fig. 6*A* and *B*). The time constants of the longest closed states would be affected most by multiple channels in the patches, and therefore, are likely to be longer in mean duration than we observed. The proportions of the closed components differed among the channels (Fig. 6*C*). The two shortest closed components (C1 and C2) are generally considered to represent intraburst closures. The relative proportions of these two components were lowest for the $\alpha1\beta3\delta$ channel, somewhat higher for the $\alpha1\beta3$ channel, and largest for the $\alpha1\beta3\gamma2L$ channel. For the $\alpha1\beta3\delta$ channel, the longer three components taken together made up most of the closures (62%), while for the other two channels the two shorter components together were predominant, making up 68% ($\alpha1\beta3$) and 76% ($\alpha1\beta3\gamma2L$) of all closures.

Burst properties. The activity of ligand-gated channels often occurs in bursts of closely grouped openings. We compared the burst properties of the three channels by defining a critical gap between the closed components C2 and C3 that represented the termination of a burst of openings. This assigned the two shortest components as intraburst closures. Distributions of burst durations and number of openings per burst were constructed and fitted with the sum of two or three exponential or geometric functions. $\alpha1\beta3\gamma2L$ channels had the longest mean burst duration, around 3-fold longer than that of $\alpha1\beta3$ and 6-fold longer than that of $\alpha1\beta3\delta$ channels (Table 1). $\alpha1\beta3\gamma2L$ channels also had the highest mean openings per burst, about 1·2-fold greater than the $\alpha1\beta3$ channels and about 2·2-fold greater than the $\alpha1\beta3\delta$ channels. The increased burst duration of the $\alpha1\beta3\gamma2L$ channels compared with the $\alpha1\beta3$ channels was due largely to the increase in the duration of openings within the burst, rather than to an increase in the number of openings per burst. The longer

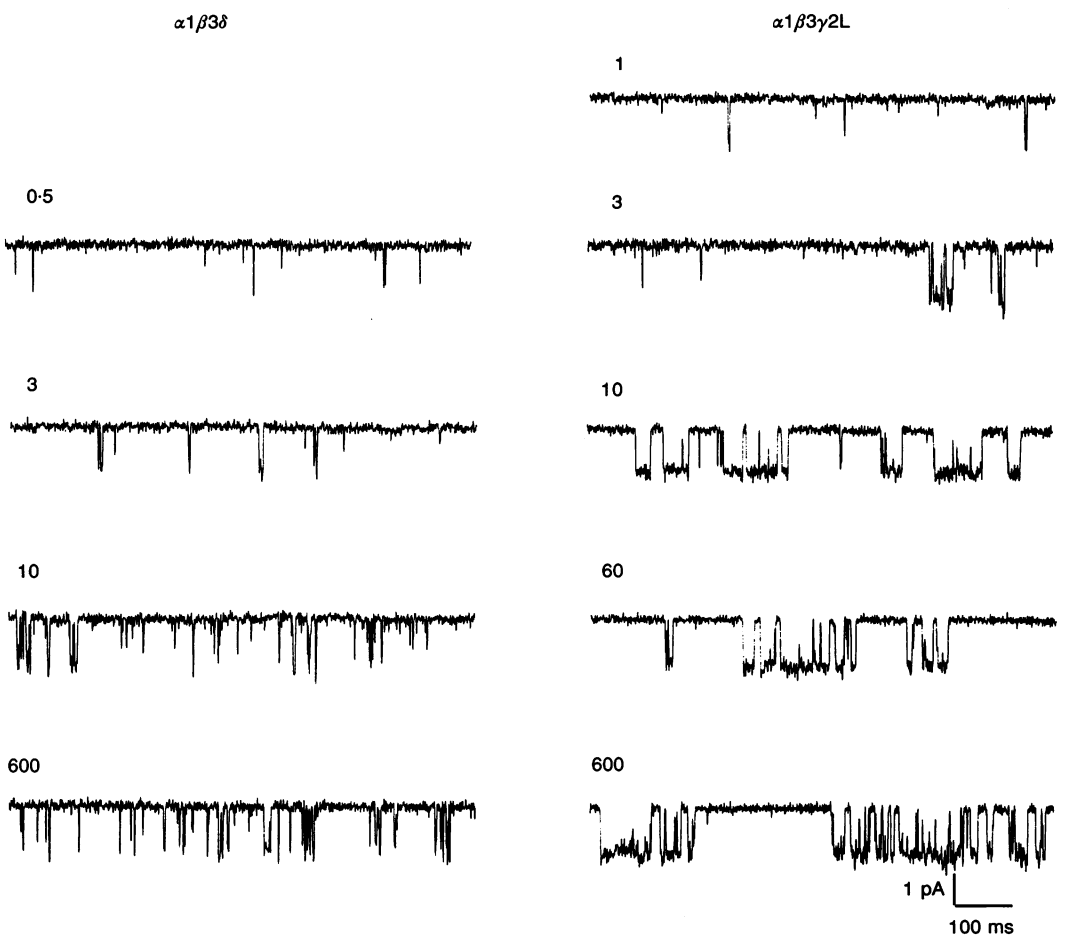

Figure 7. Effect of GABA concentration on single-channel kinetic properties

GABAR single-channel currents from outside-out patches. Traces shown were continuous 800 ms recordings from patches in response to varying concentrations of GABA, shown in μM. Not all traces were from the same patch for each isoform. The patches were held at −70 mV. For display the data were sampled at 300 μs point^{-1} and filtered at 500 Hz.

Table 2. Effect of GABA on distributions of open intervals

$\alpha1\beta3\delta$				
[GABA] (μM)	0·5	3	60	600
N	5	7	6	6
τ_1 (ms)	0·334 ± 0·067	0·301 ± 0·027	0·272 ± 0·063	0·289 ± 0·057
$Area_1$	0·903 ± 0·030	0·782 ± 0·032	0·693 ± 0·056	0·726 ± 0·043
τ_2 (ms)	1·05 ± 0·10	0·98 ± 0·18	0·931 ± 0·204	0·689 ± 0·079
$Area_2$	0·096 ± 0·030	0·217 ± 0·033	0·307 ± 0·056	0·274 ± 0·043

$\alpha1\beta3\gamma2L$					
[GABA] (μM)	1	3	10	60	600
N	5	5	8	7	6
τ_1 (ms)	0·284 ± 0·029	0·250 ± 0·024	0·270 ± 0·016	0·256 ± 0·020	0·300 ± 0·031
$Area_1$	0·880 ± 0·022	0·535 ± 0·076	0·309 ± 0·036	0·331 ± 0·044	0·220 ± 0·028
τ_2 (ms)	1·50 ± 0·18	1·02 ± 0·02	1·62 ± 0·14	1·83 ± 0·23	1·71 ± 0·30
$Area_2$	0·119 ± 0·022	0·373 ± 0·075	0·408 ± 0·059	0·377 ± 0·023	0·544 ± 0·074
τ_3 (ms)	n.a.	3·86 ± 0·545	4·77 ± 0·64	6·04 ± 0·20	4·77 ± 0·80
$Area_3$	n.a.	0·090 ± 0·02	0·282 ± 0·66	0·284 ± 0·043	0·235 ± 0·057

mean burst duration of the $\alpha1\beta3$ channels as compared with the $\alpha1\beta3\delta$ channels was due primarily to a difference in the number of openings per burst.

Effect of varying GABA concentration on $\alpha1\beta3\delta$, and $\alpha1\beta3\gamma2L$ GABAR single-channel kinetic properties

To characterize further the role of δ and $\gamma2L$ subtypes on GABAR kinetic properties, we compared the effect of GABA concentration on the distribution of openings, closings and bursts of $\alpha1\beta3\delta$ and $\alpha1\beta3\gamma2L$ channels. Single-channel currents were obtained from outside-out patches in response to concentrations of GABA varying from EC_2 to EC_{100} as calculated from the logistic equations used to fit the whole-cell concentration–response curves for each isoform (Fig. 2). For $\alpha1\beta3\gamma2L$ channels the GABA concentrations ranged from 1 μM (EC_2) to 600 μM (EC_{100}). For $\alpha1\beta3\delta$ channels the GABA concentrations ranged from 0·5 μM (EC_{12}) to 600 μM (EC_{100}). Due to the low open probability of the $\alpha1\beta3\delta$ channels, channel properties at a GABA concentration corresponding to the 1 μM GABA tested for $\alpha1\beta3\gamma2L$ channels could not be determined.

Effect of varying GABA concentration on open state properties. Increasing GABA concentration increased channel activity for both $\alpha1\beta3\gamma2L$ and $\alpha1\beta3\delta$ channels and changed the pattern of openings of the $\alpha1\beta3\gamma2L$ channel (Fig. 7). The open probability (NP_o) increased in a concentration-dependent manner (Fig. 8*A*) for both channels, although at all GABA concentrations except for the highest, the open probability of $\alpha1\beta3\delta$ channels was lower than that for $\alpha1\beta3\gamma2L$ channels. Since N was unknown, part of the differences in NP_o could have been due to consistent differences in the number of channels in the patches. Although the lower maximum current at the whole-cell level suggested that the $\alpha1\beta3\delta$ receptors were expressed with lower density, the percentages of outside-out patches that contained active channels were similar for $\alpha1\beta3\delta$ (87%) and $\alpha1\beta3\gamma2L$ (78%) isoforms. This suggested that the density of channels was similar for these isoforms. Mean open time increased with increasing GABA concentration but this increase was very slight for $\alpha1\beta3\delta$ channels (Fig. 8*B*). This suggests that for the $\alpha1\beta3\delta$ channels, the increase in NP_o was due principally to an increase in opening frequency. Open interval durations were collected for each GABA concentration for both $\alpha1\beta3\gamma2L$ and $\alpha1\beta3\delta$ channels. The distributions of open times were best fitted with the sum of two or three exponential functions. The open time histograms for the $\alpha1\beta3\delta$ channels were best fitted by the sum of only two exponential functions, regardless of the concentration of GABA (Table 2). The relative proportions of these openings shifted slightly toward an increasing occurrence of the longer open component with increasing GABA concentration, consistent with the slight increase in mean open time. For $\alpha1\beta3\gamma2L$ channels, open duration histograms were best fitted by three exponential functions at all but the lowest GABA concentration, which was fitted by two exponential functions. With increasing GABA concentration the proportions of the two longer components increased, but the time constants were unaffected (Table 2). This finding was similar to that reported for native spinal cord neuron GABARs; mean open duration increased with increasing GABA concentration due to a decrease in opening frequency of the briefest open state and an increase in opening frequency of the two longer open states (Twyman, Rogers & Macdonald, 1990). The time constants of these two shorter open states were similar for each channel, suggesting that they may share some kinetic properties, but that the $\alpha1\beta3\delta$ channel lacked the longest open state.

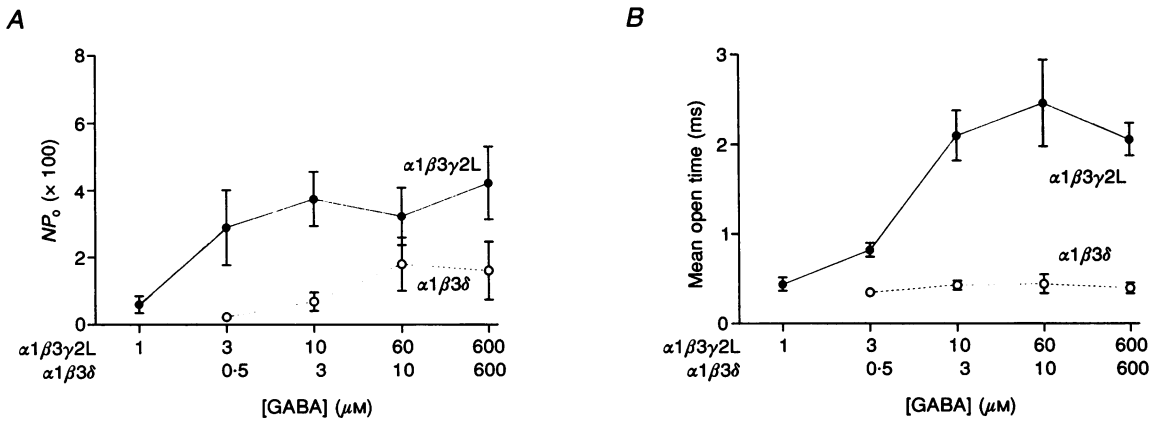

Figure 8. Effect of GABA concentration on open probability and mean open time

A, open probability (P_o) was calculated unconditionally by the total open time divided by the total time. The number of channels in each patch (N) was unknown. Points shown are the means ± S.E.M. The NP_o increased 7·8-fold from 0·5 to 10 μM GABA for the α1β3δ isoform and 8·1-fold from 1 to 600 μM GABA for the α1β3γ2L isoform. *B*, mean open times were calculated using a weighted mean of the open duration components from the fits of the open duration histograms. Points shown are means ± S.E.M.

Effect of varying GABA concentration on closed state properties. The distributions of closed intervals for both α1β3γ2L and α1β3δ channels were best fitted with the sum of five exponential functions at all GABA concentrations. The mean shut time of α1β3δ channels decreased steadily with increasing GABA concentration while that of α1β3γ2L channels initially decreased, then gradually increased (Fig. 9). This may have reflected the onset of desensitization, which was prominent in the whole-cell currents for α1β3γ2L channels but largely absent for α1β3δ channels.

The time constants of the five exponential components were similar for both α1β3γ2L and α1β3δ channels, although the longer time constants were more variable, probably because these parameters would be affected by variations in the number of channels in the patches (Table 3). The time constants of the three shorter components were generally independent of the GABA concentration. For α1β3δ channels, the time constants of the two longest closed components showed a steady decline with increasing GABA concentration. For α1β3γ2L channels, however, the time constants of these components increased with GABA concentration. This may have been due to the contribution of long duration desensitized states. With long steady-state recordings, however, desensitized, agonist-bound closed states cannot be distinguished from long closed states that represent agonist unbinding. While it is likely that at high GABA concentrations the receptor would spend little time in an unbound state, the properties of the desensitized states of these isoforms can be determined appropriately only with rapid application and removal of agonist (see Jones & Westbrook, 1995)

As GABA concentration increased, the distributions shifted towards an increasing proportion of short closures for both α1β3γ2L and α1β3δ channels. The proportions of the two

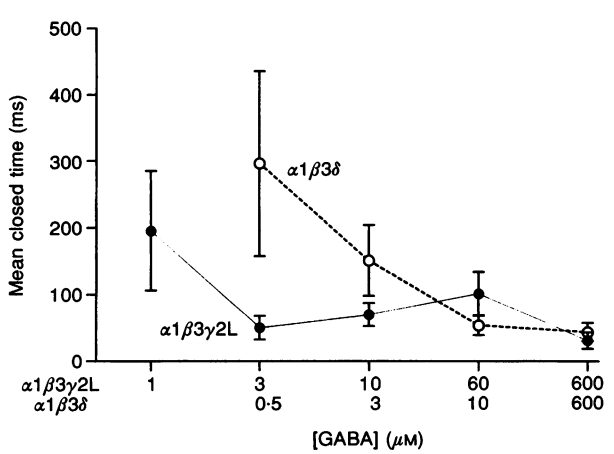

Figure 9. Effect of GABA concentration on mean closed time

Mean closed times were calculated by a weighted mean of the closed duration components from the fits of the closed duration histograms. Points shown are means ± S.E.M.

Table 3. Effect of GABA on distributions of closed intervals

$\alpha1\beta3\delta$				
[GABA] (μM)	0·5	1	3	600
N	5	7	6	6
τ_1 (ms)	0·139 ± 0·016	0·137 ± 0·08	0·207 ± 0·052	0·137 ± 0·013
$Area_1$	0·200 ± 0·030	0·248 ± 0·020	0·328 ± 0·032	0·320 ± 0·019
τ_2 (ms)	1·30 ± 0·166	2·16 ± 0·43	2·11 ± 0·42	2·05 ± 0·73
$Area_2$	0·075 ± 0·009	0·129 ± 0·022	0·172 ± 0·029	0·127 ± 0·017
τ_3 (ms)	9·68 ± 1·22	12·97 ± 2·69	12·5 ± 1·39	14·15 ± 3·78
$Area_3$	0·211 ± 0·037	0·225 ± 0·022	0·219 ± 0·033	0·334 ± 0·023
τ_4 (ms)	149·35 ± 48·65	142·4 ± 52·5	74·13 ± 14·73	77·43 ± 17·47
$Area_4$	0·256 ± 0·042	0·257 ± 0·027	0·167 ± 0·026	0·179 ± 0·024
τ_5 (ms)	972·97 ± 351·76	717·7 ± 285·6	464·37 ± 189·68	594·53 ± 285·6
$Area_5$	0·255 ± 0·067	0·138 ± 0·040	0·112 ± 0·041	0·039 ± 0·147

$\alpha1\beta3\gamma2L$					
[GABA] (μM)	1	3	10	60	6000
N	5	5	8	7	6
τ_1 (ms)	0·149 ± 0·031	0·176 ± 0·019	0·129 ± 0·014	0·144 ± 0·011	0·118 ± 0·012
$Area_1$	0·244 ± 0·051	0·507 ± 0·058	0·629 ± 0·044	0·585 ± 0·038	0·683 ± 0·05
τ_2 (ms)	0·669 ± 0·205	1·09 ± 0·170	1·56 ± 0·17	1·28 ± 0·17	0·91 ± 0·24
$Area_2$	0·101 ± 0·034	0·160 ± 0·026	0·136 ± 0·022	0·149 ± 0·013	0·146 ± 0·025
τ_3 (ms)	4·90 ± 1·49	18·86 ± 8·36	14·88 ± 1·36	11·66 ± 1·28	7·87 ± 1·90
$Area_3$	0·084 ± 0·010	0·108 ± 0·025	0·095 ± 0·012	0·108 ± 0·015	0·100 ± 0·019
τ_4 (ms)	64·40 ± 14·81	167·73 ± 72·3	145·46 ± 45·01	129·10 ± 23·2	72·2 ± 14·1
$Area_4$	0·146 ± 0·023	0·166 ± 0·047	0·098 ± 0·019	0·101 ± 0·03	0·051 ± 0·014
τ_5 (ms)	398·4 ± 131·3	1102·0 ± 758·5	1280·4 ± 795·6	2142·0 ± 852·2	1739·8 ± 678·7
$Area_5$	0·422 ± 0·068	0·0572 ± 0·024	0·041 ± 0·009	0·054 ± 0·003	0·016 ± 0·003

shorter closed components increased more dramatically for $\alpha1\beta3\gamma2L$ channels than for $\alpha1\beta3\delta$ channels. An increase in the proportions of the two short intraburst components with increasing GABA concentration was also seen with spinal cord GABARs (Twyman *et al.* 1990). This is consistent with an increase in the relative frequency of bursts of openings with increasing GABA.

Effect of varying GABA concentration on burst properties. We examined the effect of GABA on burst kinetics of both $\alpha1\beta3\gamma2L$ and $\alpha1\beta3\delta$ channels. Bursts were defined in Methods as a critical gap that separated the second and third closed components. Distributions of the burst durations were best fitted with the sum of two or three exponential functions for both isoforms. The mean burst durations increased with increasing GABA concentration (Fig. 10*A*). Distributions of the number of openings per burst were also constructed and were best fitted with the sum of two or three geometric distributions. The mean number of openings per burst also increased in a concentration-dependent manner (Fig. 10*B*). Both mean burst duration and mean openings/burst were larger for $\alpha1\beta3\gamma2L$ channels than for $\alpha1\beta3\delta$ channels regardless of the GABA concentration. These findings are similar to those reported for native spinal cord neuron GABARs; the duration and number of openings per burst of GABAR channels increased with increasing GABA concentration (Twyman *et al.* 1990).

The properties of $\alpha1\beta3\delta$ channels differed from those reported earlier for $\alpha1\beta1\delta$ channels, although detailed kinetic analysis and GABA concentration dependence were not performed in that study (Saxena & Macdonald, 1994). This suggests that the β subunit subtype may influence the single-channel kinetic properties of the channel when combined with the $\alpha1$ and δ subunits.

In some patches, 600 μM GABA appeared to cause rapid flickering, suggestive of open-channel block. Agonist-induced channel block has been reported for the nicotinic acetylcholine receptor, which is closely related to the GABAR (Ogden & Colquhoun, 1985). Patches in which this block had a clear impact on channel open time or conductance were not used in this analysis. However, the occurrence of open-channel block would have influenced the kinetic parameters measured for the response to 600 μM GABA.

These results indicate that as the GABA concentration was increased, $\alpha1\beta3\gamma2L$ channels shifted to a pattern of bursts of several long openings separated by long closed periods. This pattern was similar to that reported for native spinal cord neuron GABAR receptor channels (Twyman *et al.* 1990). For $\alpha1\beta3\delta$ channels, on the other hand, increasing GABA concentration increased the frequency of openings, but the openings still tended to occur in bursts of one or two short openings resulting in a relatively shorter open time and burst duration compared with the $\gamma2L$-containing receptor channels. Although increasing GABA concentration increased the relative frequency of the longer open state, a third component, corresponding to O3 for $\alpha1\beta3\gamma2L$ channels, was not observed with $\alpha1\beta3\delta$ channels.

DISCUSSION

We compared the functional properties of the channels formed by three different combinations of GABAR subunit subtypes ($\alpha1$ and $\beta3$, $\alpha1$, $\beta3$ and δ, and $\alpha1$, $\beta3$ and $\gamma2L$ subtypes). The heterodimeric receptor composed of $\alpha1$ and $\beta3$ subtypes alone exhibited many of the functional properties associated with GABARs. The receptor has been shown to be sensitive to GABA with more than one agonist binding site and contains the binding sites for many GABAR-specific allosteric modulators, including barbiturates, picrotoxin, neurosteroids and loreclezole, but not for benzodiazepines (Sieghart, 1995). The $\alpha1\beta3$ subtypes formed a chloride permeable channel which exhibited complex kinetic properties, including multiple open and closed states and rapid desensitization. Addition of the $\gamma2$ or δ subtype to $\alpha1$ and $\beta3$ subtypes to form heterotrimeric GABARs changed the functional properties of the channel. The $\gamma2L$ subtype altered the responsiveness of the cell to GABA and the amount of current produced. Both subtypes appeared to affect whole-cell desensitization properties. Addition of either a $\gamma2L$ or δ subtype to the $\alpha1$ and $\beta3$ subtypes increased the single-channel conductance. The single-channel kinetic properties were also altered by the $\gamma2L$ and δ subtypes, although in different ways.

Effect of subunit subtype composition on single-channel GABAR conductance

Addition of either a γ or δ subtype to the $\alpha1$ and $\beta3$ subtypes increased the single-channel conductance compared with the $\alpha1\beta3$ receptor, suggesting that each contributed to the conduction pathway. There is strong evidence that regions surrounding the second transmembrane domain (TM2) of GABAR subunits play an important role in determining the conductance and ionic selectivity of the channel pore (Smith & Olsen, 1995). Comparison of the amino acid sequences of these regions for the $\alpha1$, $\beta3$, $\gamma2$ and δ subtypes is shown in Fig. 11. Interestingly, the δ subtype contains no charged residues in the short intracellular loop between TM1 and TM2, while the $\alpha1$ and $\gamma2$ subtypes contain both positively and negatively charged residues, for a net charge of zero. The $\beta3$ subtype has a negatively charged glutamic acid, which could contribute to a lower chloride conductance for the channel. Mutagenesis of the positively charged residue introduced rectification of the whole-cell current–voltage relationship, suggesting that this region can influence conductive properties (Backus *et al.* 1993). $\gamma2$ and δ subtypes contain three positively charged residues in the extracellular loop between TM2 and TM3, although only two positions are conserved. While the stoichiometry of the $\alpha\beta$ receptor is unknown, at least one α and/or β subunit must be replaced to form the heterotrimeric receptor. Both $\gamma2$ and δ subtypes contribute a net charge of +4 in the regions spanning the end of TM1 to the beginning of TM3, adding one positive charge for each α subunit replaced, and two positive charges for each β subunit replaced. This could account for the increased conductance of the $\alpha\beta\gamma$ and $\alpha\beta\delta$ GABAR channels.

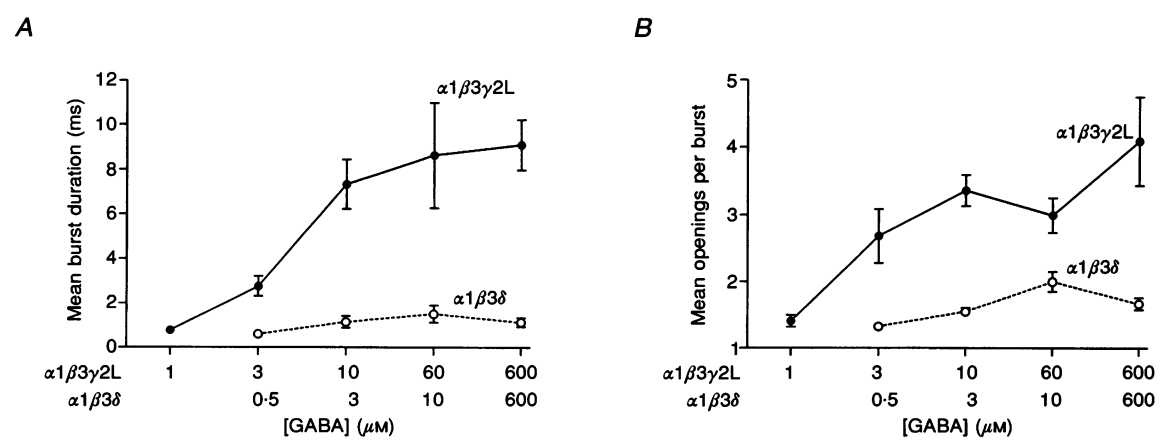

Figure 10. Effect of GABA on burst properties

A, mean burst durations were calculated by a weighted mean of the burst duration components from the fits of the burst-duration histograms. Histograms were best fitted by the sum of two or three exponential functions. Points shown are means ± S.E.M. *B*, mean openings/burst were calculated by a weighted mean of the openings/burst components from the fits of the openings/burst histograms. Histograms were best fitted by the sum of two or three geometric functions. Points shown are means ± S.E.M.

Effect of receptor composition on single-channel kinetic properties

The $\alpha1\beta3$, $\alpha1\beta3\delta$ and $\alpha1\beta3\gamma2L$ channels exhibited different kinetic properties but also shared a few common features. Since the shape of the concentration–response relationships for GABA were similar, with Hill slopes greater than 1, two or more binding sites for GABA are probably appropriate for all three channels.

The $\alpha1\beta3$ channel exhibited at least two open states and five closed states. Channel openings occurred in a pattern of bursts of several openings separated by long closures. At a concentration of GABA near the EC_{50}, long closures were frequently observed. This may have represented entry into a desensitized state(s), as desensitization was prominent in the whole-cell record for the $\alpha1\beta3$ isoform, but could also represent closures due to agonist unbinding. The $\alpha1\beta3$ channel entered two short duration open states.

Addition of the δ subtype to form $\alpha1\beta3\delta$ had little effect on the open state properties of the channel compared with those of the $\alpha1\beta3$ channel. Two open states were observed, with similar time constants and relative proportions to those of the $\alpha1\beta3$ channel. Increasing the GABA concentration increased the relative proportion of the longer open state, indicating that the transition between the open states included a GABA-dependent step. The kinetic properties of the $\alpha1\beta3\delta$ channel differed from those of the $\alpha1\beta3$ channel primarily in the characteristics of the closed components. At the whole-cell level, $\alpha1\beta3\delta$ currents showed little desensitization. This was reflected in the single-channel kinetic properties as with increasing GABA concentration the channel open probability steadily increased, and the time constants of the longer closed components steadily decreased. The burst kinetics of the $\alpha1\beta3\delta$ and $\alpha1\beta3$ channels also differed. The $\alpha1\beta3$ channels had a greater mean number of openings per burst, suggesting that the tendency to enter the short intraburst closures was greater for the $\alpha1\beta3$ channel than for the $\alpha1\beta3\delta$ channel.

In contrast to the δ subunit, addition of the $\gamma2L$ subtype altered the single-channel kinetic properties of both the open and closed intervals compared with $\alpha1\beta3$ channels. The kinetic properties of the $\alpha1\beta3\gamma2L$ channel were very similar to those reported for the native spinal cord GABAR channels (Twyman *et al.* 1990). Three open states were observed, and the relative proportions of the longer open states increased with increasing GABA concentration, suggesting a GABA binding step was present between the open states. The increase in mean burst duration and openings per burst with increasing GABA concentration also suggests that the burst structure of the recombinant GABAR channel was similar to that of native spinal cord GABAR channels, with the longer open states contributing the multi-opening bursts. In contrast to the findings of Twyman *et al.* (1990), we found that the shortest closed component (C1) increased more consistently with GABA concentration than the second shortest component (C2). They found that both these components increased proportionally, and suggested that all the open states accessed the intraburst closures with the same relative frequency. Our results suggest that the longer open states enter C1 more frequently than C2. Our analysis of the burst structure was not as detailed, and this variation may be due to differences in the receptor subunit composition, recording conditions, or number of intervals analysed. The increased duration of the long closed components with increasing GABA concentration was consistent with entry into desensitized states.

While it is difficult to determine the structural basis for channel gating, a few general conclusions can be drawn from our results. The heterodimeric $\alpha1\beta3$ channel contributes the structure required for at least two short-lived open states and several closed states. Addition of the δ subunit to form the $\alpha1\beta3\delta$ channel had little effect on the open state properties of the channel, and principally altered the entry into the intraburst and long duration closed states. The $\gamma2L$ subunit, however, changed the channel gating kinetics dramatically. With the addition of the $\gamma2L$ subunit, the

TM1	Intracellular	TM2	Extracellular	TM3	
..SFWI	SQA	AVPA**R**VSLGITTVLTMTTLMVSA	**R**SSLP**R**ASAI**K**	ALD..	δ
		+1	+3		net = +4
..SFWI	N**K**D	AVPA**R**TSLGITTVLTMTTLSTIA	**RK**SLP**K**VSYVT	AMD..	γ
	+1/−1	+1	+3		net = +4
..SFWL	N**R**E	SVPA**R**TVFGVTTVLTMTTLSISA	**R**NSLP**K**VAYAT	AMD..	$\alpha1$
	+1/−1	+1	+2		net = +3
..SFWI	NY**D**	ASAA**R**VALGITTVLTMTTINTHL	**RE**TLP**K**IPYV**K**	AID..	$\beta3$
	−1	+1	−1/+3		net = +2

Figure 11. Sequence comparison of GABAR subunits

Amino acid alignment of the putative second transmembrane domain (TM2) of rat δ, $\gamma2$, $\alpha1$, and $\beta3$ subunits (from Tyndale, Olsen & Tobin, 1995). The complete TM2 sequence, the last four amino acids of TM1 and the first three amino acids of TM3 are boxed. Charged amino acids are shown in bold type, and positively charged amino acids are in bold and underlined. The total charges for the TM2 domain and the intracellular and extracellular regions surrounding it are shown beneath each sequence and the net charge for all these sequences for each subunit are shown on the far right.

channel was able to enter a long-lived open state (O3). The γ2L subunit, but not the δ subunit, contributed to the formation of this stable open conformation.

The regional expression of mRNA for γ and δ subunits is different, with only a few regions of the brain expressing neither family (Shivers *et al.* 1989; Wisden *et al.* 1992). The different kinetic properties of the $\alpha1\beta3$, $\alpha1\beta3\delta$, and $\alpha1\beta3\gamma2L$ channels would be expected to alter the synaptic response to release of GABA. The low mean open time and open probability of the single $\alpha1\beta3$ and $\alpha1\beta3\delta$ channels could account for the relatively low current observed at the whole-cell level in transfected cells and would result in a lower amplitude synaptic response when compared with synapses expressing the same number of $\alpha1\beta3\gamma2L$ receptors. The shorter burst duration of the $\alpha1\beta3\delta$ channel may result in a shorter duration synaptic current. The lack of a large degree of desensitization for this channel could also allow greater responsiveness to repetitive stimuli. An accurate prediction of the kinetic properties of the synaptic currents of these different isoforms would require a more complete kinetic model than we currently have available, including information from both rapid application and steady-state analysis.

Angelotti, T. P., Uhler, M. D. & Macdonald, R. L. (1993). Assembly of $GABA_A$ receptor subunits: analysis of transient single-cell expression utilizing a fluorescent substrate/marker gene technique. *Journal of Neuroscience* **13**, 1418–1428.

Angelotti, T. P. & Macdonald, R. L. (1993). Assembly of $GABA_A$ receptor subunits: $\alpha_1\beta_1$ and $\alpha_1\beta_1\gamma_{2s}$ subunits produce unique ion channels with dissimilar single-channel properties. *Journal of Neuroscience* **13**, 1429–1440.

Backus, K. H., Arigoni, M., Drescher, U., Scheurer, L., Malherbe, P., Möhler, H. & Benson, J. A. (1993). Stoichiometry of a recombinant $GABA_A$ receptor deduced from mutation-induced rectification. *NeuroReport* **5**, 285–288.

Chen, C. & Okayama, H. (1987). High-efficiency transformation of mammalian cells by plasmid DNA. *Molecular and Cellular Biology* **7**, 2745–2752.

Colquhoun, D. & Sakmann, B. (1985). Fast events in single-channel currents activated by acetylcholine and its analogues at the frog muscle end-plate. *Journal of Physiology* **369**, 501–557.

Dominguez-Perrot, C., Feltz, P. & Poulter, M. O. (1996). Recombinant $GABA_A$ receptor desensitization: the role of the $\gamma2$ subunit and its physiological significance. *Journal of Physiology* **497**, 145–159.

Draguhn, A., Verdoorn, T. A., Ewert, M., Seeburg, P. H. & Sakmann, B. (1990). Functional and molecular distinction between recombinant rat $GABA_A$ receptor subtypes by Zn^{2+}. *Neuron* **5**, 781–788.

Greenfield, L. J. Jr & Macdonald, R. L. (1996). Whole cell and single channel $\alpha1\beta1\gamma2s$ $GABA_A$ receptor currents elicited by a 'multipuffer' drug application device. *Pflügers Archiv* **432**, 1080–1090.

Greenfield, L. J. Jr, Sun, F., Neelands, T. R., Burgard, E. C., Donnelly, J. L. & Macdonald, R. L. (1997). Expression of functional $GABA_A$ receptors in transfected L929 cells isolated by immunomagnetic bead separation. *Neuropharmacology* **36**, 63–73.

Horn, R. (1987). Statistical methods for model discrimination. Applications to gating kinetics and permeation of the acetylcholine receptor channel. *Biophysical Journal* **51**, 255–263.

Huggenvik, J. I., Collard, M. W., Stofko, R. E., Seasholtz, A. F. & Uhler, M. D. (1991). Regulation of the human enkephalin promoter by two isoforms of the catalytic subunit of cyclic adenosine 3′,5′-monophosphate-dependent protein kinase. *Molecular Endocrinology* **5**, 921–930.

Jones, M. V. & Westbrook, G. L. (1995). Desensitized states prolong $GABA_A$ channel responses to brief agonist pulses. *Neuron* **15**, 181–191.

Krishek, B. J., Amato, A., Connolly, C. N., Moss, S. J. & Smart, T. G. (1996). Proton sensitivity of the $GABA_A$ receptor is associated with the receptor subunit composition. *Journal of Physiology* **492**, 431–443.

Laurie, D. J., Seeburg, P. H. & Wisden, W. (1992*a*). The distribution of 13 $GABA_A$ receptor subunit mRNAs in the rat brain. II. Olfactory bulb and cerebellum. *Journal of Neuroscience* **12**, 1063–1076.

Laurie, D. J., Wisden, W. & Seeburg, P. H. (1992*b*). The distribution of thirteen $GABA_A$ receptor subunit mRNAs in the rat brain. III. Embryonic and postnatal development. *Journal of Neuroscience* **12**, 4151–4172.

Macdonald, R. L. & Angelotti, T. P. (1993). Native and recombinant $GABA_A$ receptor channels. *Cellular Physiology and Biochemistry* **3**, 352–373.

McManus, O. B. & Magleby, K. L. (1988). Kinetic states and modes of single large-conductance calcium-activated potassium channels in cultured rat skeletal muscle. *Journal of Physiology* **402**, 79–120.

Ogden, D. C. & Colquhoun, D. (1985). Ion channel block by acetylcholine, carbachol and suberyldicholine at the frog neuromuscular junction. *Proceedings of the Royal Society* B **225**, 329–355.

Porter, N. M., Angelotti, T. P., Twyman, R. E. & Macdonald, R. L. (1992). Kinetic properties of $\alpha1\beta1$ γ-aminobutuyric $acid_A$ receptor channels expressed in chinese hamster ovary cells: regulation by pentobarbital and picrotoxin. *Molecular Pharmacology* **42**, 872–881.

Saxena, N. C. & Macdonald, R. L. (1994). Assembly of $GABA_A$ receptor subunits: role of the δ subunit. *Journal of Neuroscience* **14**, 7077–7086.

Saxena, N. C. & Macdonald, R. L. (1996). Properties of putative cerebellar γ-aminobutyric $acid_A$ receptor isoforms. *Molecular Pharmacology* **49**, 567–579.

Shivers, B. D., Killisch, I., Sprengel, R., Sontheimer, H., Köhler, M., Schofield, P. R. & Seeburg, P. H. (1989). Two novel $GABA_A$ receptor subunits exist in distinct neuronal subpopulations. *Neuron* **3**, 327–337.

Sieghart, W. (1995). Structure and pharmacology of γ-aminobutyric $acid_A$ receptor subtypes. *Pharmacological Reviews* **47**, 181–234.

Sigworth, F. J. & Sine, S. M. (1987). Data transformations for improved display and fitting of single-channel dwell time histograms. *Biophysical Journal* **52**, 1047–1054.

Smith, G. B. & Olsen, R. W. (1995). Functional domains of $GABA_A$ receptors. *Trends in Pharmacological Science* **16**, 162–168.

Twyman, R. E., Rogers, C. J. & Macdonald, R. L. (1990). Intraburst kinetic properties of the $GABA_A$ receptor main conductance state of mouse spinal cord neurones in culture. *Journal of Physiology* **423**, 193–220.

Tyndale, R. F., Olsen, R. W. & Tobin, A. J. (1995). $GABA_A$ receptors. In *Ligand- and Voltage-gated Ion channels*, ed. North, R. A., pp. 265–290. CRC Press, Boca Raton, USA.

VERDOORN, T. A., DRAGUHN, A., YMER, S., SEEBURG, P. H. & SAKMANN, B. (1990). Functional properties of recombinant rat $GABA_A$ receptors depend upon subunit composition. *Neuron* **4**, 919–928.

WISDEN, W., LAURIE, D. J., MONYER, H. & SEEBURG, P. H. (1992). The distribution of 13 $GABA_A$ receptor subunit mRNAs in the rat brain. I. Telencephalon, diencephalon, mesencephalon. *Journal of Neuroscience* **12**, 1040–1062.

Acknowledgements

This work was supported by NIH grants RO1-NS33300 (R.L.M.) and T32-NS07222 (J.L.F.)

Author's email address

R. L. Macdonald: rlmacd@umich.edu

Received 17 January 1997; accepted 6 August 1997.